IL NUOVO CIMENTO Vol. 37 C, N. 1 Gennaio-Febbraio 2014
DOI 10.1393/ncc/i2014-11682-9

Colloquia: IFAE 2013

AMS-02: Status and first results

M. Duranti(*) for the AMS Collaboration
INFN Sezione Perugia - Via Pascoli, 06123 Perugia, Italy

ricevuto l'1 Ottobre 2013

Summary. — The AMS experiment has been deployed onboard the International Space Station on 19 May 2011 to perform accurate measurements of the cosmic radiation. In this contribution we will briefly discuss the characteristics of the detector and present the first results: the precision measurement of the positron fraction in primary cosmic rays (CR) in the energy range from 0.5 to 350 GeV.

PACS 96.50.sb – Composition, energy spectra and interactions.
PACS 96.50.S- – Cosmic Rays.
PACS 95.35.+d – Dark matter (stellar, interstellar, galactic, and cosmological).
PACS 07.87.+v – Spaceborne and space research instruments, apparatus, and components (satellites, space vehicles, etc.).

1. – Introduction

The Alpha Magnetic Spectrometer, AMS-02, is a general-purpose high-energy particle physics detector. It was launched into space with the Space Shuttle STS-134 mission and installed onboard the ISS on 19 May 2011 to conduct a unique long-duration mission (about 20 years) of fundamental physics research in space. The accurate measurement of the antimatter components in Cosmic Rays (CR) is the main experimental challenge of this spectrometer conceived for the quest of primordial anti-matter, as witnessed by the presence of antihelium or heavier antinuclei, or possible excesses of light antimatter (positrons, antiprotons, antideuterons) and gammas coming from exotic sources, as dark-matter annihilation. Precision measurements of the CR composition and energy spectra up to the TeV scale and their variation with time due to the solar activity are also in the AMS-02 scientific plan and will allow to better understand the sources and propagation mechanisms of CR in our galaxy.

In this contribution we will focus our discussion on the AMS-02 precision measurement of the positron fraction in CR in the energy range 0.5–350 GeV [1] based on about 6.8 million $e^{\pm}$ selected in the first 18 months of operation.

(*) E-mail: matteo.duranti@pg.infn.it

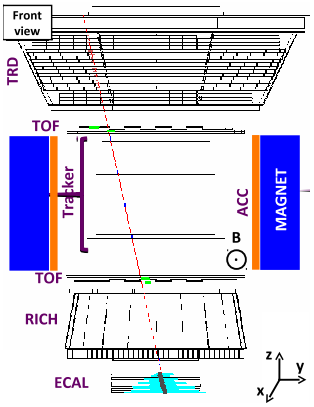

Fig. 1. – A 660 GeV electron measured by the AMS detector on the ISS in the bending (y-z) plane. Tracker planes measure the particle charge and momentum. The TRD identifies the particle as an electron. The TOF measures the charge and ensures that the particle is downward-going. The RICH independently measures the charge and velocity. The ECAL, measuring the 3D shower profile, independently identifies the particle as an electron, and measures its energy.

The well-established mechanism at the origin of the CR positron components is their secondary production in the inelastic interactions of CR nuclei with the interstellar gas. This corresponds to a small positron component (about 10% of the total electron flux) rapidly decreasing with energy. Excesses in the positron abundance with respect to the expected flux, as recently measured by PAMELA [2] and FERMI [3], could then give an indication of new sources either of astrophysical origin or from dark-matter annihilation. Only an accurate measurement of this excess over an extended energy range can give the experimental clues to establish its origin.

In the following, we will briefly introduce the AMS-02 detector and its capability in positron identification, the data sample and the analysis method will be then reviewed. We will conclude with the discussion of the result.

2. – The AMS-02 detector

The layout of the AMS-02 detector [1, 4] is shown in fig. 1. It consists of 9 planes of microstrip silicon detectors acting as Tracker; a gaseous Transition Radiation Detector (TRD); 4 planes of plastic scintillators acting as Time of Flight and main trigger (TOF); a permanent Magnet; an array of anti-coincidence counters (ACC), surrounding the Magnet bore; a Ring Imaging Čerenkov detector (RICH); and an Electromagnetic Calorimeter (ECAL). The figure also shows a 660 GeV electron detected by AMS.

The $e^{\pm}/p$ separation and the charge sign assessment to distinguish e^{+} from the e^{-} are the experimental challenges in the positron fraction measurement. The combined TRD, ECAL and Tracker measurements are used to reject the overwhelming proton background. The TRD and ECAL are separated by the Magnetic field volume: secondary particles produced in the TRD or upper TOF material are mostly swept away and either do not enter the ECAL or are identified by the tracker. The TRD is designed to use transition radiation to distinguish between $e^{\pm}$ and protons, and $\mathrm{d}E/\mathrm{d}x$ to independently identify nuclei. It consists of 5248 proportional tubes of 6 mm diameter arranged in 20 layers interleaved with a 20 mm thick fibre fleece radiator. In order to differentiate between $e^{\pm}$ and protons, signals from the 20 layers are combined in a TRD estimator

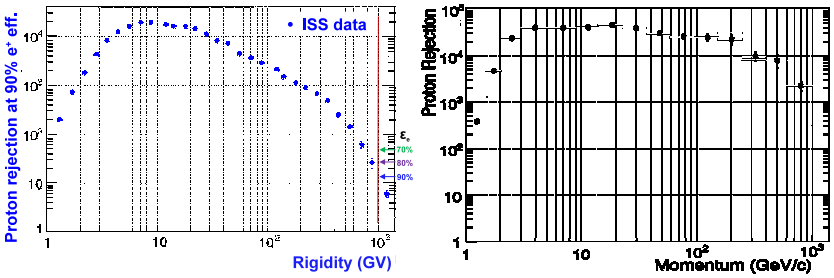

Fig. 2. – Left: The proton rejection measured by the TRD as a function of track momentum at 90% selection efficiency for $e^{\pm}$. The proton rejection power can be readily improved by reducing the $e^{\pm}$ efficiency: this is shown quantitatively at 1 TeV, as an example. Right: The measured proton rejection using ECAL and Tracker. For 90% $e^{\pm}$ ECAL selection efficiency, the measured proton rejection is about 10000, in the momentum range 3–500 GeV/c.

formed from the ratio of the log-likelihood probability of the $e^{\pm}$ hypothesis to that of the proton hypothesis. The proton rejection power of the TRD estimator at 90% $e^{\pm}$ efficiency measured on orbit is 10^3 to 10^4, as shown in fig. 2, left.

The ECAL consists of a multilayer sandwich of 98 lead foils and about 50000 scintillating fibres with an active area of $648 \times 648\,\mathrm{mm}^2$ and a thickness of 166.5 mm corresponding to 17 radiation lengths. The calorimeter is composed of 9 superlayers, with the fibres running in one single direction. The 3-D imaging capability of the detector is obtained by stacking alternate superlayers with fibres parallel to the x and y axes alternatively (5 and 4 superlayers, respectively). The energy resolution of the ECAL is parametrized as a function of energy (in GeV) as $\sigma(E)/E = \sqrt{(0.104)^2/E + (0.014)^2}$. The proton rejection power of the ECAL estimator when combined with the independent measurement of the particle momentum (p) from the Tracker ($E/p > 0.75$) reaches about 10000 (see fig. 2, right), as determined from the ISS data.

The Tracker accurately determines the trajectory and absolute charge (Z) of cosmic rays by multiple measurements of the coordinates and energy loss. The spatial resolution of each plane is measured to be better than 10 μm in the bending direction and the charge resolution is $\Delta Z = 0.06$ at $Z = 1$. A Maximum Detectable Rigidity, of 2 TV is provided by the spectrometer for $Z = 1$ particles, this allows to clearly distinguish e^- from e^+ introducing only a minor uncertainty in the positron fraction measurement due to charge sign confusion (CC). Energy/momentum matching allows to crosscheck and reject the events with wrong rigidity reconstruction.

3. – Analysis procedure

Over 25 billion events have been analyzed. Optimisation of all reconstruction algorithms was performed using test beam data and ISS data (identifying, for example, clean control samples for ECAL (TRD) by means of independent TRD (ECAL) and Tracker selection).

Monte Carlo simulated events are produced using a dedicated program developed by the AMS Collaboration which is based on the GEANT-4.9.4 package [5]. This program simulates electromagnetic and hadronic interactions of particles in the materials of AMS and generates detector responses. The digitization of the signals, including those of the AMS trigger, is simulated precisely according to the measured characteristics of the electronics. The digitized signals then undergo the same reconstruction used for data.

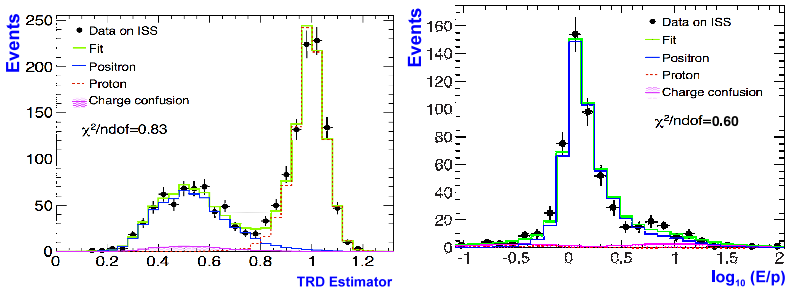

Fig. 3. – The 2-dimensional reference spectra for $e^{\pm}$ and background are fitted to data in the plane (TRD estimator-log(E/p)). Here are shown, as example, in the 83.2–100 GeV energy bin and for the positive selected data sample. Separation power against the proton background of the TRD estimator is shown on the left panel. Separation power against the charge confused electrons of the E/p matching is shown on the right panel.

In this analysis events are selected by requiring a track in the TRD and in the Tracker, a cluster of hits in the ECAL and a measured velocity $\beta \sim 1$ in the TOF consistent with a downward-going $Z = 1$ particle. In order to reject more than 99% of the remaining protons, an energy-dependent cut on the ECAL estimator is applied. To reject, instead, positrons and electrons produced by the interaction of primary cosmic rays with the atmosphere [6], the energy measured by the ECAL is required to exceed by a factor of 1.2 the maximal Störmer cutoff [7] at the geomagnetic location where the particle was detected, for either a positive or a negative particle and at any angle within the AMS acceptance. The selection efficiency for positrons and electrons is estimated to be about 90% in the acceptance of the ECAL. Any charge asymmetry in the selection efficiency is important only at $E < 3$ GeV and has been accounted for in the systematics. The remaining sample contains about 6800000 primary positrons and electrons and about 700000 protons. The composition of the sample versus energy is determined by the TRD estimator and the E/p matching.

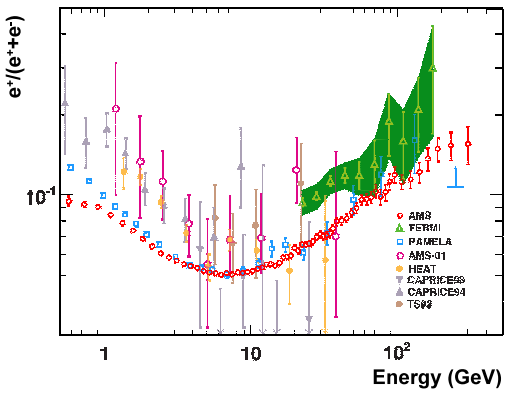

Fig. 4. – The positron fraction compared with the measurements from PAMELA [2], Fermi-LAT [3] and others previous experiments [8-11]. The error bars for AMS are the quadratic sum of the statistical and systematic uncertainties and the horizontal positions are the centers of each bin.

The positron fraction is determined in ECAL energy bins. The binning is chosen according to the energy resolution and the high available statistics such that migration of the signal events to neighbouring bins has a negligible contribution to the systematic errors above about 2 GeV. The migration uncertainty was obtained by folding the measured rates of positrons and electrons with the ECAL energy resolution.

In every energy bin, the 2-dimensional reference spectra for $e^{\pm}$ and the background are fitted to data in the plane (TRD estimator-log(E/p)).

Results of a fit for the positive sample in the range 83.2–100 GeV are presented in fig. 3 as a projection onto the TRD estimator axis (left) and as a projection onto the E/p one (right). The charge confusion contribution is from electrons misidentified as positrons.

There are several sources of systematic uncertainty including those associated with the asymmetric acceptance of e^+ and e^-, the selection of $e^{\pm}$, bin-to-bin migration, the reference spectra knowledge and charge confusion. The systematic uncertainties were examined in each energy bin over the entire spectrum from 0.5 to 350 GeV. In the final result the systematic uncertainties are summed in quadrature with the statistical ones.

4. – Results and conclusions

The measured positron fraction is presented in fig. 4 as a function of the reconstructed energy at the top of the AMS detector, together with results from previous experiments. The accuracy of AMS-02 and the high statistics available enable the reported AMS-02 positron fraction spectrum to be clearly distinguishable from earlier measurements. As seen in the figure, below 10 GeV the positron fraction decreases with increasing energy as expected from the e^+ secondary production. At higher energy, a steady increase of the positron fraction is observed from 10 to about 250 GeV, which continues at higher energy with a different slope. This is not consistent with a purely secondary production of positrons [12]. The expected improvement both on the systematics and the statistical uncertainties along the AMS-02 mission will allow to better investigate the high energy behaviour.

* * *

This work has been supported by acknowledged person and institutions in [1]. The author wishes to thank the colleagues in AMS-02 and in particular B. Bertucci for the careful reading of the manuscript. This work has been partially supported by ASI (Italian Space Agency) under contract ASI-INFN I/002/13/0.

REFERENCES

[1] Aguilar M. *et al.*, *Phys. Rev. Lett. A*, **110** (2013) 141102, DOI:10.1103/PhysRevLett.110.141102.
[2] Adriani O. *et al.*, *Nature*, **458** (2009) 607, DOI:10.1038/nature07942.
[3] Ackermann M. *et al.*, *Phys. Rev. Lett.*, **108** (2012) 011103, DOI:10.1103/PhysRevLett.108.011103.
[4] Lübelsmeyer K. *et al.*, *Nucl. Instrum. Methods Phys. Res. Sec. A*, **654** (2011) 639, DOI:10.1016/j.nima.2011.06.051; Kirn Th., *Nucl. Instrum. Methods Phys. Res. Sec. A*, **706** (2013) 43, DOI:10.1016/j.nima.2012.05.010; Rosier-Lees S. *et al.*, *J. Phys. Conf. Ser.*, **404** (2012) 012034, DOI:10.1088/1742-6596/404/1/012034.
[5] Agostinelli S. *et al.*, *Nucl. Instrum. Methods Phys. Res. Sec. A*, **506** (2003) 250, DOI:10.1016/S0168-9002(03)01368-8.

[6] Alcaraz J. *et al.*, *Phys. Lett. B*, **484** (2000) 10, DOI:10.1016/S0370-2693(00)00588-8.
[7] Störmer C., *Q.J.R. Meteorol. Soc*, **82** (1956) 115, DOI:10.1002/qj.49708235123.
[8] Golden R. L. *et al.*, *Astrophys. J.*, **457** (1996) L103, DOI:10.1086/309896.
[9] Boezio M. *et al.*, *Adv. Space Res.*, **27** (2001) 669, DOI:10.1016/S0273-1177(01)00108-9.
[10] Beatty J. J. *et al.*, *Phys. Rev. Lett.*, **93** (2004) 241102, DOI:10.1103/PhysRevLett.93.241102.
[11] Aguilar M. *et al.*, *Phys. Lett. B*, **646** (2007) 145, DOI:10.1016/j.physletb.2007.01.024.
[12] Serpico P. D., *Astropart. Phys.*, **39-40** (2012) 2, DOI:10.1016/j.astropartphys.2011.08.007.